Journal of the European Ceramic Society **18** (1998) 543–552

PII: S0955-2219(97)00160-X
0955-2219/98/$19.00 + 0.00

Aluminum-Containing Ytterbium Nitrogen Woehlerite Solid Solutions. Synthesis, Structure, and some Properties

V. A. Ijevskii,* U. Kolitsch, H. J. Seifert, I. Wiedmann and F. Aldinger

Max-Planck-Institut für Metallforschung, Pulvermetallurgisches Laboratorium, D-70569 Stuttgart, Germany and Universität Stuttgart, Institut für Nichmetallische Anorganische Materialien, Heisenbergstrasse 5, D-70569 Stuttgart, Germany

(Received 3 June 1997; accepted 11 August 1997)

Abstract

A complete solid solution between $Yb_4Si_2O_7N_2$ (ytterbium nitrogen woehlerite) and $Yb_4A1_2O_9$ with general formula $Yb_4Si_{2-x}Al_xO_{7+x}N_{2-x}$ has been established by pressureless sintering at 1670–1700°C. X-ray powder diffraction patterns of intermediate members reveal a pronounced tetragonal pseudosymmetry. Unit cell parameters increase in a non-linear way with increasing alumina content. Weight loss of the solid solutions increases with increasing Al/Si ratio on heating in the temperature range 1950–2000°C under 1 bar nitrogen pressure which implies partial decomposition of the formed aluminates, although the temperature at which the thermal decomposition begins, rises at the same time. Coarsening of the microstructure was observed with the increase of the amount of alumina dissolved. Oxidation resistance of the solid solutions improves considerably with higher alumina content. Thus, alumina-containing nitrogen woehlerite solid solutions may be considered as favourable secondary grain boundary phases in Si_3N_4-based ceramics.

1 Introduction

Silicon nitride-based ceramics have been intensively studied for many years and are used for high-temperature structural applications owing to the favourable combination of chemical and mechanical properties in a wide temperature range. However, dense Si_3N_4 components cannot be produced by means of a classical solid-state sintering process. Complete densification of silicon nitride is possible only by the addition of oxide sintering aids. As a result, dense silicon nitride materials consist of highly refractory β-Si_3N_4 grains, or a mixture of α- and β-Si_3N_4 ones, separated by less refractory vitreous phases. The high-temperature behaviour of Si_3N_4 materials primarily depends on the amount, distribution and chemical composition of the amorphous intergranular phases which are basically RE silicates and/or aluminates. Definite improvement of the high-temperature properties can be achieved by intergranular phase crystallisation.[1–4] However, this possibility is known to be of limited effectiveness.

An alternative approach to secondary phase tailoring in silicon nitride ceramics, namely sialons, was proposed very recently.[5–10] There it was stated that nitrogen melilite-based solid solutions containing Al_2O_3, designated M^{SS} ($RE_2Si_{3-x}Al_xO_{3+x}N_{4-x}$, with RE = La to Lu, and Y, and $x \leq 1$), can serve as an excellent alternative to the traditional oxysilicates in the role of secondary intergranular phases. However, the secondary phases that were produced by these authors were not phase pure nitrogen melilite solid solutions (M^{SS}), but rather a mixture of phases, one of them being nitrogen woehlerite, $RE_4Si_2O_7N_2$, and its Al_2O_3 doped solid solution. Furthermore, the Al_2O_3 solubility limits in nitrogen melilite solid solutions were reported to decrease with decreasing RE^{3+} ionic radii. No solid solubility was observed for RE = Yb.[7,10]

The most recent publication on RE–melilite solid solutions[10] covers not only formation conditions and stability of both pure RE–melilites and their Al_2O_3-containing solid solutions for a number of RE elements with varying ionic radii but also outlines systematic trends in the solid solubility,

*To whom correspondence should be addressed (on leave from the Institute for Problems of Materials Science, National Academy of Sciences of Ukraine, Kiev, Ukraine).

unit cell dimensions, and the competition with neighbouring phases. The latter are rationalised in terms of ionic size effects and acid-base reactions and summarised in a series of tentative phase diagrams. It was also clearly shown, which is of primary interest in regard of the present work, that the stability of alumina-containing RE woehlerite solid solutions increases with the decrease of RE ionic radius.

Nitrogen woehlerites (N–woehlerites), also known as J-phases, are compounds with the general formula $RE_4Si_2O_7N_2$, where RE = La to Lu, and Y. These phases were discovered relatively early in the course of silicon nitride development[11] but together with N–melilites, general formula $RE_2Si_3O_3N_4$, they were not considered as promising secondary phases due to their poor oxidation resistance at temperatures exceeding 1000°C.[12] Under such conditions cristobalite and rare earth silicates are formed which causes a volume expansion of up to ~30% resulting in catastrophic failure of the material. However, the alumina-containing N–melilite solid solutions show very good oxidation resistance.[5–9] Additionally, they crystallise readily on cooling from the liquid phase thus providing both higher rate and extent of crystallisation than in the case of devitrification of glasses by means of post-sintering heat treatments or controlled cooling.[6] Moreover, and which is of high value from the standpoint of potential application, these phases do not form low-temperature eutectics with the Si_3N_4 matrix and have much better refractoriness in general (melting points lie in the temperature range 1780–1850°C[6]).

Only Y-containing N–woehlerite, $Y_4Si_2O_7N_2$, was thoroughly investigated and described in regard of structure and some properties. Complete solid solution with $Y_4Al_2O_9$ was reported.[11] Full and consistent structural characterisation of $Y_4Si_2O_7N_2$ was accomplished only recently and it was proven that it is isostructural with the monoclinic mineral cuspidine $Ca_4Si_2O_FF_2$.[13] All the other N–woehlerites were subjected to only marginal scrutiny and are normally referred to as isostructural compounds.

The present paper focuses on structural characterisation and thermal properties of Yb–nitrogen woehlerite, $Yb_4Si_2O_7N_2$, and its Al_2O_3-containing solid solutions. Properties of the solid solutions were investigated in order to evaluate their suitability as alternative grain boundary phases in Si_3N_4-based ceramics for high-temperature applications.

2 Experimental

Pure Yb–N–woehlerite $Yb_4Si_2O_7N_2$ and three Al_2O_3-containing solid solutions with general formula $Yb_4Si_{2-x}Al_xO_{7+x}N_{2-x}$, where $x = 0{\cdot}33$, 1, and 1·33 (i.e. with Si/Al ratios of 2/1, 1/1, and 1/2), as well as $Yb_4Al_2O_9$ (YbAM) were synthesised from Si_3N_4 (>98% α-Si_3N_4; GP 14/13, Starck Germany), Yb_2O_3 (99·5% purity; Ventron, Germany), Al_2O_3 (99·99% purity; AKP-30, Sumitomo Chemical Corp., Japan), and SiO_2 (>99·8% purity; Aerosil 2000, Degussa, Germany) powders. Corrections as to oxygen content in the silicon nitride powder were made in the compositional calculations. Mixtures were prepared by attrition milling in dehydrated ethanol with Si_3N_4 milling media for 4 h with subsequent drying in a rotation evaporator and sieving. Cylindrical samples (14·5 mm diameter and 12 mm height) were prepared by cold isostatic pressing under 630 MPa.

Sintering, with the exception of YbAM, was performed in a gas-pressure furnace with graphite heating element (Astro Industries, Santa Barbara, USA) under slight (0·2–0·3 MPa) overpressure of 99·99% pure nitrogen. Samples were placed in individual BN crucibles with a powder bed identical to the composition of the samples. Sintering temperatures varied between 1650 and 1700°C. Holding time varied from 2 up to 72 h. Sintering periods of at least 4 h were necessary to obtain equilibrium.

$Yb_4Al_2O_9$ (YbAM) was synthesised by firing a pellet of a proper composition in air at 1700°C on a Yb_2O_3 powder bed two times for a period of 50 h with intermediate grinding.

The sintered materials were subsequently characterised by X-ray diffraction (XRD) and scanning electron microscopy (SEM). XRD was carried out on a Siemens D5000 powder diffractometer (position-sensitive detector, Ni-filtered Cu K_α, radiation, measuring range 6 to 80° 2Θ, step width 0·02 2Θ, counting time 20 s). Phases were identified using data available in JCPDS Powder Diffraction file (PDF).[14] For XRD of powdered specimens, 99·999% pure silicon was used as an internal standard. Indexing and unit cell refinements were done with the least-square refinement program of Benoit[15] which is a PC version of the well-known Appleman and Evans software.[16] The SEM examinations were performed with a Cambridge S200 (Cambridge Instruments, UK) with an attached WDX analyser Microspec 2A. The samples were prepared by standard ceramographic procedure which included multistage polishing by diamond tools with or without subsequent plasma etching (Plasma Barrel Etcher PT 7150, Bio-Rad, UK).

Thermal stability of the synthesised compounds was determined by means of simultaneous (DTA/TG) thermal analysis (STA 501, Bähr, Germany). Temperature was measured with an optical pyrometer. Samples were placed into BN crucibles. Calibration with the melting point of 99·99% pure

Al_2O_3 was done directly prior to our measurements. A heating rate of 10 K min^{-1} from RT up to 1200°C and of 1 K min^{-1} from 1200 to 2100°C, with an inverse cooling schedule, were applied.

Differential scanning calorimetry (DSC; model 'Multi-Detector High-Temperature Calorimeter' equipped with a DSC detector with upper temperature limit 1400°C; Setaram, France) was used to characterise a synthesised $Yb_4Al_2O_9$ sample. A Pt crucible and 99·999% pure Ar atmosphere were used for the DSC investigations. Heating and cooling rates were 1 and 5 K min^{-1}. The calibration of the instrument was done immediately prior to the DSC runs by measuring the melting point of 99·99 + % pure Au.

High-temperature oxidation investigations were carried out by means of continuous thermogravimetry (STA 501, Bähr, Germany) between 700 and 1400°C in air, both in non-isothermal (heating rate 2–10 K min^{-1}) and isothermal conditions. The former was used to determine the starting temperature of active oxidation and the general oxidation behaviour of all materials. The isothermal oxidation experiments were conducted at 720 ± 5°C for 10 h, thus ensuring complete oxidation of the samples which was confirmed by subsequent XRD investigations.

3 Results and Discussion

3.1 Solid solution along the series $Yb_4Si_2O_7N_2$–$Yb_4Al_2O_9$

All sintered samples (sintering temperature 1680–1700°C) with compositions conforming to pure $Yb_4Si_2O_7N_2$ and to $Yb_4Si_{2-x}Al_xO_{7+x}N_{2-x}$ solid solutions with x = 0·33, 1, and 1·33 (i.e. with Si/Al ratios of 2/1, 1/1, and 1/2) were phase-pure compounds according to their XRD patterns (Fig. 1). The YbAM sample showed some impurities of the Barnet phase. Weight losses during sintering were negligible. This is considered evidence for the existence of a complete solid solution between $Yb_4Si_2O_7N_2$ and $Yb_4Al_2O_9$ which is comparable to the one observed for the Y analogues.[17] Refined unit cell parameters of the compounds are presented and compared to available literature values in Table 1 and as a diagram shown in Fig. 2.

X-ray powder diffraction data for $Yb_4Si_2O_7N_2$ were recently given by Nishimura and Mitomo as part of an investigation of the system Si_3N_4–SiO_2–Yb_2O_3.[18] However, these X-ray data display a rather large systematic error (which can be easily seen when comparing observed with calculated d-spacings). Additionally, the space group is given as $P2_1/m$ (instead of $P2_1/c$, see discussion below) and the *a* and *c* cell parameters were inverted. The erroneous space group assignment may explain the somewhat large difference between the *c* cell parameters of the $Yb_4Si_2O_7N_2$ sample of Nishimura and Mitomo and of our sample (Table 1).

The XRD patterns of the intermediate solid solutions (Fig. 1) display the same pseudo-tetragonal symmetry that has been observed for the solid solution series $Y_4Si_2O_7N_2$–$Y_4Al_2O_9$.[17] Severe X-ray reflection overlap is caused by the mentioned pseudo-symmetry. Progressing from $Y_4Si_2O_7N_2$, an increasing Al_2O_3 content resulted in an increasing overlap. The most striking overlap is observed for the sample with an Si/Al ratio of 1/2

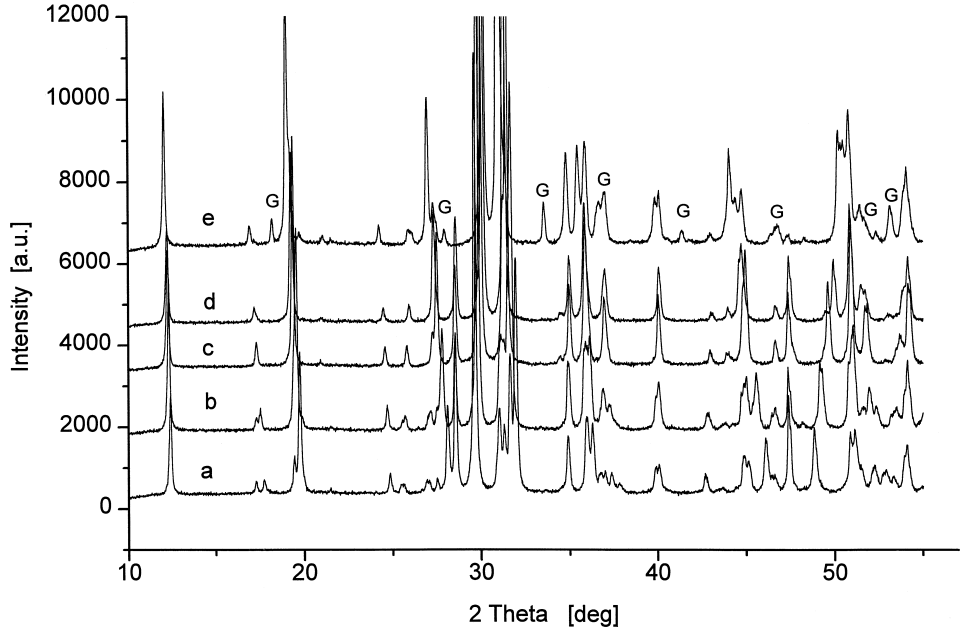

Fig. 1. Comparison of XRD patterns along the solid solutions series $Yb_4Si_2O_7N_2$–$Yb_4Al_2O_9$. 'G' designates the impurity garnet phase $Yb_3Al_5O_{12}$ in the pattern of $Yb_4Al_2O_9$.

Table 1. Refined unit cell parameters of pure $Yb_4Si_2O_7N_2$, solid solutions $Yb_4Si_{2-x}Al_xO_{7+x}N_{2-x}$ and pure $Yb_4Al_2O_9$, compared with existing literature data

Compound[a]	*a[Å]*	*b[Å]*	*c[Å]*	β[Å]	*V [Å³]*	*Reference no.*
$Yb_4Si_2O_7N_2$[b]	7·47	10·32	10·77	111·3	774	[11]
$Yb_4Si_2O_7N_2$[b,c]	7·456	10·299	10·712	110·56	770·2	[18]
$Yb_4Si_2O_7N_2$	7·459(1)	10·300(2)	10·739(3)	110·85(2)	771·0(2)	This work
$Yb_4Si_{2-xAl_x}O_{7+x}N_{2-x}$ $x=0{\cdot}66$ (Si/Al = 2/1)	7·416(2)	10·295(2)	10·841(4)	110·50(3)	775·3(3)	This work
$Yb_4Si_{2-x}Al_xO_{7+x}N_{2-x}$, $x=1$ (Si/Al = 1/1)	7·348(2)	10·280(2)	10·911(6)	109·65(3)	776·2(4)	This work
$Yb_4Si_{2-x}Al_xO_{7+x}N_{2-x}$, $x=1.33$ (Si/Al = 1/2)	7·310(5)	10·333(9)	10·935(17)	108·98(12)	781(1)	This work
$Yb_4Al_2O_9$	7·257(2)	10·313(3	11·033(4)	108·46(3)	783·3(3)	This work
$Yb_4Al_2O_9$[b]	7·278	10·310	11·040	108·30	786·5	[32, 42]
$Yb_4Al_2O_9$	7·2636(3)	10·3375(4)	11·0256(5)	108·293(3)	786·0	[41]

[a]Listed in order of decreasing Si/Al ratio.
[b]No standard deviations given in original papers.
[c]Indexing of the original powder data is wrongly based on space group $P2_1/m$.[18] Therefore, *a* and *c* have been interchanged here to conform to space group $P2_1/c$.

($Yb_4Si_{0·66}Al_{1·33}O_{8·33}N_{0·66}$); its XRD data are listed in Table 2. For instance, the 'sharp' reflection at d = 2·865 Å in the XRD pattern of $Yb_4Si_{0·66}Al_{1·33}O_{8·33}N_{0·66}$ (see pattern d in Fig. 1) is actually consisting of at least four reflections (Table 2). By contrast, the XRD pattern of the silicon- and nitrogen-free solid solution end member, $Yb_4Al_2O_9$, exhibits a larger number of better resolved peaks (see pattern e in Fig. 1).

According to Thompson,[17] the pronounced tetragonal pseudo-symmetry of intermediate members in the solid solution series $Y_4Si_2O_7N_2$–$Y_4Al_2O_9$ mentioned above arises from the fact that Y_4SiAlO_8N (Si/Al ratio 1/1) can be described as pseudotetragonal with $a = 10{\cdot}5$ and $c = 3{\cdot}$Å. Similarly, $Y_4Al_2O_9$ may be characterised by

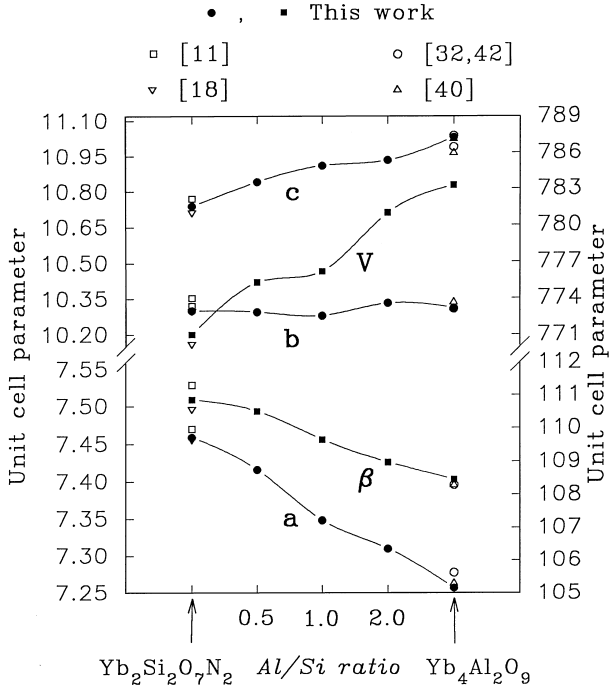

Fig. 2. Graphic representation of the unit cell parameter change along the solid solution series $Yb_4Si_2O_7N_2$–$Yb_4Al_2O_9$.

$a = 10{\cdot}363$ and $c = 3{\cdot}738$ Å. The following relationships are valid: $a_{tetr} = c_{mon} = c_{mon}\sin\beta \sim 10{\cdot}5$ A, and $c_{tetr} = 1/2a_{mon} = c_{mon}\cos\beta \sim 3{\cdot}8$. By analogy, the ytterbium solid solution member Yb_4AlSiO_8N may be described as pseudotetragonal with $a = 10 \cdot 28$ and $c = 3{\cdot}67$Å.

Not much is known about the low-temperature stability of $RE_4Si_2O_7N_2$ phases. Therefore, low temperature stability tests by means of annealing in N_2 (normal pressure) for up to 100 h at 1250 and 1350°C were performed. It was observed that both pure Yb woehlerite and its alumina-containing solid solutions are stable in the above temperature range.

3.2 Possible O/N and A/Si ordering schemes

Figure 2 illustrates that the variation of unit cell parameters with composition is not linear, as has also been reported for the solid solution series $Y_4Si_2O_7N_2$–$Y_4Al_2O_9$.[17] Obviously, there is a minimum of the unit cell volume *V* at Si/Al ~1/1. Volume contraction in solid solutions usually indicates a deviation from perfect solid solution behaviour. In our case, this volume minimum may indicate some Al/Si and/or O/N ordering which would result in a denser packing and thus in a reduced cell volume. On the other hand, no superstructure reflections (which would indicate complete ordering) were observed for all solid solution samples. In this respect, however, one should bear in mind that the X-ray diffraction pattern characteristics of the solid solutions are dominated by the strong scattering power of the heavy Yb^{3+} cation in the structure. Superstructure reflections may have an intensity too low to be observed by usual laboratory XRD.

Recent Rietveld refinement of the structure of pure yttrium nitrogen woehlerite, $Y_4Si_2O_7N_2$, yielded no clear details on O/N ordering in this phase.[13] It was proposed that the structure contains either

Table 2. Indexed X-ray data for the pseudotetragonal solid solution $Yb_4Si_{2-x}Al_xO_{7+x}N_{2-x}$, $x = 1{\cdot}33$ (Si/Al ratio 1/2), illustrating the extreme X-ray reflection overlap

$Yb_4Si_{2-x}Al_xO_{7+x}N_{2-x}$, $x = 1{\cdot}33$[a]			
d_{obs}(Å)	d_{calc}(Å)	I	hkl
7·312	7·310	23	011
5·179	5·172	4	002
4·625	4·625	41	012
	4·622		021
3·651	3·655	3	022
3·447	3·446	4	−211
3·276	3·279	27	−210
(b)	3·271		013
3·261	3·268	7	031
(b)	3·260		−212
2·979	2·984	98	−221
2·865	2·873	100	−220
(b)	2·868		023
	2·867		032
	2·860		−222
	2·855		−213
2·597	2·594	2	221
2·570	2·575	16	−223
2·510	2·507	29	−231
(b)	2·506		041
−2·499 (s)	2·494	6	132
2·435	2·437	13	033
(b)	2·432		−232
	2·427		123
2·252	2·262	13	231
(b)	2·250		310
	2·249		−233
2·103	2·105	2	320
(b)	2·102		142
2·060 (b)	2·065	3	−242
2·033	2·034	15	232
2·028	2·027	19	051
1·9494	1·953	4	321
(b)	1·949		−243
−1·924	1·919	1	052
1·913	1·916	1	330
(b)	1·912		151
1·829	1·827	15	−402
1·796	1·800	28	−251
(b)	1·799		331
	1·794		152
1·776	1·776	9	−411
(b)	1·775		322
	1·774		250
1·702	1·705	4	410
(s,b)	1·702		−421
	1·702		251
1·695	1·697	8	−423
	1·696		−253
1·629	1·630	2	161
(b)	1·628		−162
1·612	1·614	1	−432
1·596	1·597	11	−431
(b)	1·593		−433
1·573	1·572	2	351
1·553	1·555	7	162
(b)	1·552		−163
1·549(s)	1·548	7	421
1·542	1·542	21	260
1·538(s)	1·539	16	−350
1·533(s)	1·534	7	−353

[a]Space group $P2_a/c$, refined unit cell parameters: $a = 7{\cdot}310(5)$, $b = 10{\cdot}333(9)$, $c = 10{\cdot}935(17)$Å, $\beta = 108{\cdot}98(12)°$, $V = 781(1)$Å^3 (compare Table 1); (b) = broad, (s) = shoulder of adjacent reflection.

$Si_2O_5N_2$ or Si_2O_6N ditetrahedral units with N atoms occupying the bridging position.[13] This confirms the general observation that N prefers bonds with Si whereas O is preferentially bonded to some larger metal cation.[19]

The Rietveld data for $Y_4Si_2O_7N_2$[13] may be compared to structural information for $Nd_4Si_2O_7N_2$ deduced by infrared absorption data which were measured by Baraton *et al.*[20] Absorption bands of the $Nd_4Si_2O_7N_2$ sample were not as sharp as those of $Nd_2Si_3O_3N_4$, an N–melilite, for which neutron diffraction studies showed the oxygen and nitrogen atoms to be perfectly ordered[20] and therefore it was inferred that $Nd_4Si_2O_7N_2$ may have a disordered structure.

Several possible ordering schemes may be envisaged in the $Yb_4Si_{2-x}Al_xO_{7+x}N_{2-x}$ solid solutions. There may, first, be O/N ordering, or, second, Al/Si ordering, or, third, a combination of both. In the $Y_4Si_2O_7N_2$ (and probably also $Yb_4Si_2O_7N_2$) structure, there are three distinct O/N sites.[13] The substitution $Si^{4+} + N^{3-} = Al^{3+} + O^{2-}$ may influence the distribution of O and N on these sites. The substitutional Al^{3+} ions may prefer one of the two Si sites in the $Y_4Si_2O_7N_2$ structure, although both sites have very similar environments.[13]

Electron diffraction using a transmission electron microscope could prove useful in verifying if there are observable superstructure reflections in these solid solutions. Neutron diffraction studies might be able to accurately determine possible Al/Si and/or O/N ordering.

From a thermodynamic point of view, complete O/N and/or Al/Si disordering would probably produce an entropy gain of the structure which would result in an increased stability. (Dis)ordering may therefore also depend on temperature.

3.3 General discussion of the relation between $RE_4Si_2O_7N_2$ and $RE_4Al_2O_9$

Our observation of a complete solid solution between $Yb_4Si_2O_7N_2$ and $Yb_4Al_2O_9$ requires a general discussion of $RE_4Si_2O_7N_2$ compounds, their crystal chemistry, and their relation to $RE_4Al_2O_9$ compounds. It has been reported that $RE_4Si_2O_7N_2$ compounds are stable for the complete range of rare earth elements from RE = La to Lu, and Y.[11,12,17,18,21–26] They were first prepared by Marchand *et al.* for RE = La, Nd, Sm, Gd, Dy, Ho, Er, Yb, and Y.[11] Guha[22] and Montorsi and Appendino[26] showed that Ce-, Pr-, Tm-, and $Lu_4Si_2O_7N_2$ fit well into this series.

Most authors agree that $RE_4Si_2O_7N_2$ compounds crystallise in the monoclinic space group $P2_1/c$ and are isostructural with the mineral cuspidine, $Ca_4Si_2O_7F_2$, and structurally similar to woehlerite, $NaCa_2(Zr,Nb)Si_2O_8(O,OH,F)$, and

other related mineral phases.[27] The space group of $Y_4Si_2O_7N_2$ and its isotypism with cuspidine were recently confirmed by MacKenzie *et al.*[13] The lanthanum member, $La_4Si_2O_7N_2$, may, however, exhibit a slightly different symmetry, as was assumed earlier.[28] Single crystal structure analysis of $La_4Si_2O_7N_2$, using Precession and Weissenberg techniques, indicated space group $P2_1/m$.[29,30] On the other hand, complete solid solution was reported along the join $La_4Si_2O_7N_2$–$Y_4Si_2O_7N_2$.[31]

In parts of grown $La_4Si_2O_7N_2$ single crystals, Ii *et al.*[29] observed twin lamellae which were attributed to thermal stress. However, this observation may indicate that $RE_4Si_2O_7N_2$ compounds show a similar modular structural behaviour as cuspidine, woehlerite and related mineral phases.[27] The structure of these mineral phases may be visualised as an arrangement of different modules which gives rise to slightly different space groups and disorder phenomena like domain structure, micro-scale twinning, and stacking faults (see Ref. 27 for more details).

The possibility of solid solution formation between $RE_4Si_2O_7N_2$ and $RE_4Al_2O_9$ via a coupled substitution mechanism $Si^{4+} + N^{3-} = Al^{3+} + O^{2-}$ has already been suggested in 1976 by Marchand *et al.*[11] The solid solution can be considered quite probable since both end members are isostructural, crystallising in the same space group ($P2_1/c$).

To our knowledge, there have been no investigations of other joins $RE_4Si_2O_7N_2$–$RE_4Al_2O_9$ except for RE = Y[17] and Yb (this work). Further work in this area is necessary, since $RE_4Al_2O_9$ compounds are only stable for RE = Nd to Lu,[32–34] but $RE_4Si_2O_7N_2$ compounds for RE = La to Lu. Thus, it may be assumed that in $RE_4Si_2O_7N_2$ phases with RE = La to Pr, no or only limited amounts of Al_2O_3 can be dissolved. During an investigation of the system Sm–Si–Al–O–N, Sun *et al.*[35] tried to obtain a $Sm_4Si_2O_7N_2$-based solid solution containing 2·55 mass% Al_2O_3. Since these authors did not observe visible differences in d-values compared to pure $Sm_4Si_2O_7N_2$, they deduced that no solid solution is formed in this case.

Starting from the $RE_4Al_2O_9$ composition, it may seem probable that in the (unstable) $RE_4Al_2O_9$ compounds for RE = La to Pr, a replacement of (Al + O) with (Si + N) has a stabilising effect which would possibly result in stable $RE_4Al_2O_9$-based solid solutions. $Nd_4Al_2O_9$, which is only stable in a small temperature range at high temperatures,[34] may show a temperature-dependent solid solution range.

Concerning the solid solution between $RE_4Si_2O_7N_2$ and $RE_4Al_2O_9$, it is interesting to note that, according to recent investigations in our laboratory, $Gd_4Al_2O_9$, $Y_4Al_2O_9$, $Yb_4Al_2O_9$, and possibly all other known $RE_4Al_2O_9$ phases exhibit a large SiO_2 solubility in the range of about 15–20 mol% SiO_2.[36,37]

3.4 Some properties of the $Yb_4Si_{2-x}Al_xO_{7+x}N_{2-x}$ solid solutions

Attempts to determine the melting points of the Yb–woehlerite and its Al_2O_3-containing solid solutions by means of high temperature STA in nitrogen atmosphere did not produce the desired results. The heating of the samples in the above conditions caused intensive thermal decomposition of all investigated samples. As a result, the initial composition shifts to either ytterbium oxide or a mixture of the latter with ytterbium aluminates as presented in Table 3. Therefore, one can not ascribe the measured melting point (melting occurred for all Al_2O_3-containing materials at about 1970 ± 20°C) to the initial material. The observed behaviour is consistent with the known one for other oxynitrides at high temperatures under normal nitrogen pressure.[17]

The registered weight loss values together with final phase composition determined by X-ray and chemical analysis indicate that not only nitrogen is removed from the material but also silicon, most probably in the form of silicon monoxide (SiO), similar to the mechanism of silicon nitride-based materials thermal decomposition under the same thermal and environmental conditions. In our case, the formation of highly volatile SiO can be additionally promoted by the graphite environment of the furnace as it was observed for silicon nitride based materials.[38]

Moreover, the measured weight loss exceeds the calculated values in case if the thermal decomposition of the compounds in question occurred according to the following generalised scheme:

Table 3. High temperature decomposition along the solid solution series $Yb_4Si_2O_7N_2$–$Yb_4Al_2O_9$[a]

Initial compound	*Temperature of the beginning of thermal decomposition (°C)*	*Decomposition products*[b]
$Yb_4Si_2O_7N_2$	1580 ± 5	Yb_2O_3, $Yb_4Si_2O_7N_2$ (traces)
$Yb_4Si_{2-x}Al_xO_{7+x}N_{2-x}$, $x = 0{\cdot}33$	1615 ± 5	Yb_2O_3, $Yb_4Al_2O_9$
$Yb_4Si_{2-x}Al_xO_{7+x}N_{2-x}$, $x = 1$	1625 ± 5	Yb_2O_3, $Yb_4Al_2O_9$
$Yb_4Si_{2-x}Al_xO_{7+x}N_{2-x}$, $x = 1{\cdot}33$	1680 ± 10	Yb_2O_3, $Yb_4Al_2O_9$

[a]Measured by STA at 1 K min^{-1} under flowing N_2.
[b]Determined by XRD; confirmed by chemical analysis.

$$Yb_4Si_2O_7N_2 \rightarrow Yb_2O_3 + SiO\uparrow + N_2\uparrow \quad (1)$$

$$Yb_4Si_{2-x}Al_xO_{7+x}N_{2-x} \rightarrow Yb_2O_3 + Yb_4Al_2O_9 + SiO\uparrow + N_2\uparrow \quad (2)$$

In all cases weight loss exceeded 30% while the maximum possible weight loss for pure woehlerite which contains the highest amount of both Si and N was calculated to be 29·9%. The value of measured weight loss for pure woehlerite is reasonably close (32%) to the calculated one. The slightly higher value may be explained by some measurement error. In the case of solid solutions with alumina the weight loss lies in the range of 40–46% and can not be accounted for in the same way. Obviously, the presence of alumina increases the weight loss at high temperatures, although at the same time the temperatures at which the thermal decomposition starts are somewhat elevated (Table 3).

The most plausible explanation of this effect can be provided if a parallel is drawn with the known effect of weight loss in yttrium garnet and other yttrium aluminates via sublimation from the solid state or evaporation of the melt of Al-containing gaseous species occurring at temperatures in excess of 1850°C.[39] The ytterbium aluminates being similar with yttrium ones in regard of the properties could exhibit the same behaviour, although at slightly higher temperatures which is again to be expected on account of the higher refractoriness of Yb aluminates. In view of our results the available data on the melting points of Al_2O_3-containing nitrogen melilites $RE_2Si_{3-x}Al_xO_{3+x}N_{4-x}$ which were reported to lie in the range of 1780–1850°C[5–9,18] seem to be of arguable nature, since the conditions of the experiments, nitrogen pressure in particular, were not specified. Both N–melilites and N–woehlerites should behave similar in this temperature range and one would reasonably expect the thermal decomposition of melilites prior to melting.

From the standpoint of the determined homogeneity range Yb- and $Y_4Si_{2-x}Al_xO_{7+x}N_{-x}$ solid solutions have the advantage that there exists a complete solid solution range (x =0–2) and therefore a widely adjustable O/N ratio, whereas for the N-melilite solid solutions $RE_2Si_{3-x}Al_xO_{3+x}N_{4-x}$ the maximum value of x is merely 1.

Recently, reversible and possibly martensitic phase transformations of $RE_4Al_2O_9$ compounds (with volume shrinkage of 0·5–0·7% on heating and with thermal hysteresis) have been described.[40] In the case of $Yb_4Al_2O_9$, the transformation was reported at ≈1300°C using a heating rate of 10 K min^{-1}. A high-temperature DSC run of our $Yb_4Al_2O_9$ sample (1·13 g powder) confirmed this transformation, although at a slightly lower temperature. During heating at 1 K min^{-1} a small endothermic peak at around 1280 ± 15°C was observed. A corresponding small exothermic peak appeared in the cooling curve at 1274 ± 5°C. Using heating and cooling rates of 5 K min^{-1} enhanced the peaks (Fig. 3) which were then observed at ca 1263 ± 15°C on heating and at 1276 ± 10°C on cooling (temperature values are corrected for influence of heating rate). It was noted that in all measurements the peak on heating was broader and less defined than the peak on cooling. The minor difference between our average transformation temperatures (≈1277°C) and the value previously given (≈1300°C[40]) might be attributed to both different heating rates and purity of starting powders.

Microstructures of $Yb_4Si_{2-x}Al_xO_{7+x}N_{2-x}$(except $Yb_4Al_2O_9$) fired at 1680°C for 4 h were investigated by SEM. All samples exhibit a relatively coarse microstructure with equiaxial, rounded grains [Fig. 4(a)–(d)]. With rising Al/Si ratio, the average grain size increases from about 1 μm for pure $Y_4Si_2O_7N_2$ to about 5 μm for the solid solution member with $x = 1{\cdot}33$. At the same time, the porosity remained roughly on the same level of 14–15% while the average pore size increased with the Al/Si ratio. Further densification presented some problems. With improved density achieved by sintering at higher temperatures (1720–1740°C), excessive liquid phase formation occurred which resulted both in local inhomogeneities and a compositional gradient in the samples due to loss of nitrogen in the outer layer of the fired bodies. Porosity reduction will pose no problem when nitrogen woehlerite solid solutions are present as secondary phases in Si_3N_4-based ceramics.

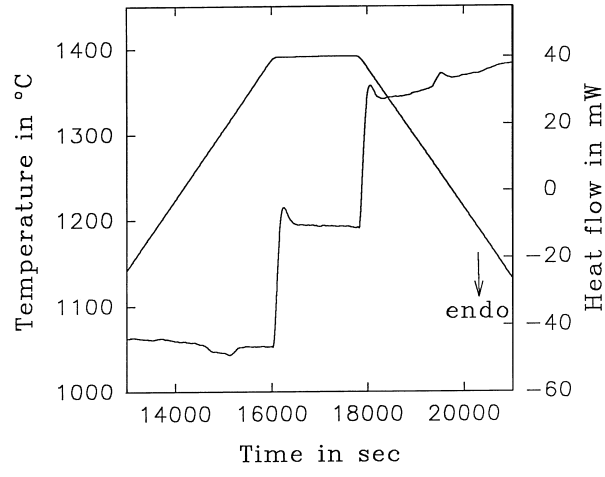

Fig. 3. High-temperature DSC curve of $Yb_4Al_2O_9$ using heating and cooling rates of 5 K min^{-1}. The peaks near ~1277°C are caused by a reversible phase transformation.

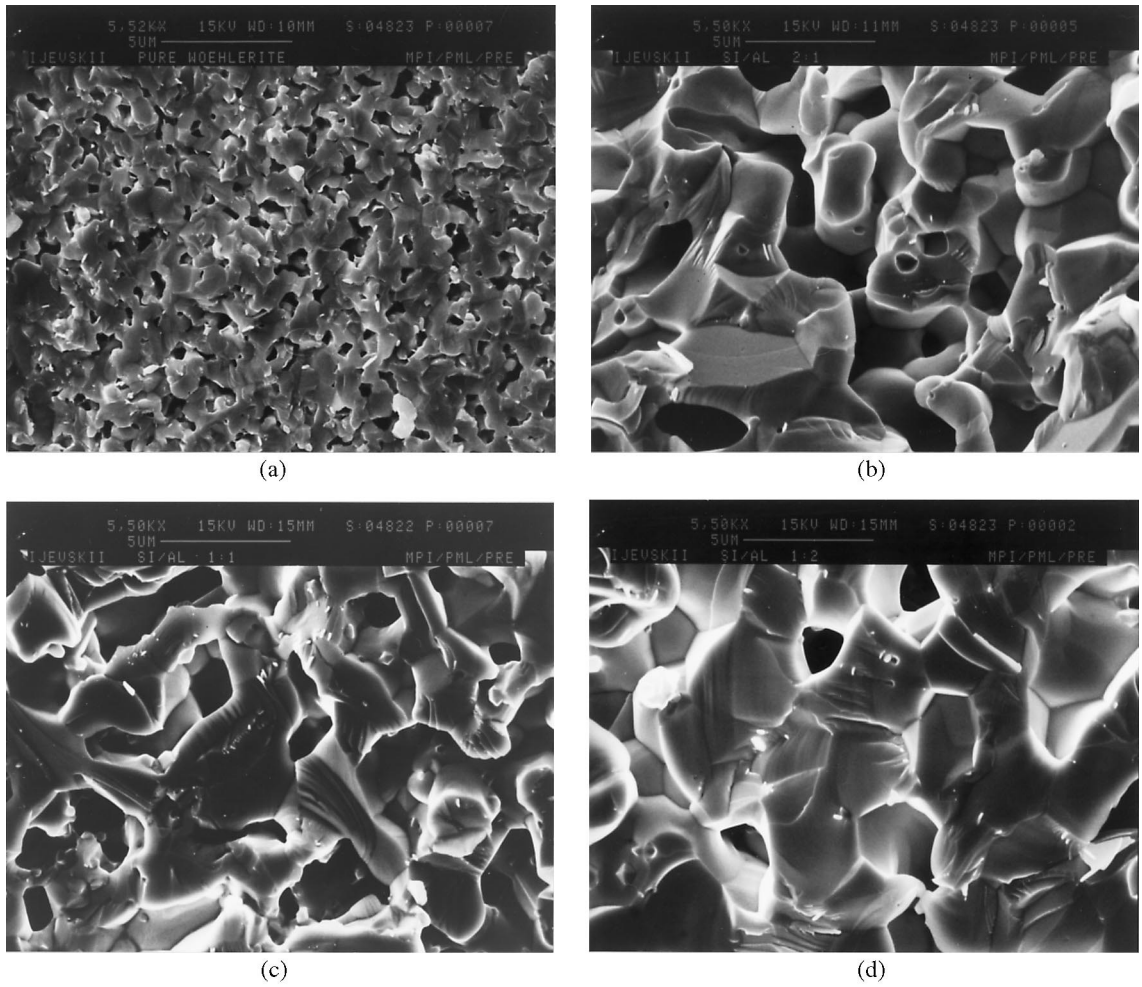

Fig. 4. Microstructure of $Yb_4Si_{2-x}Al_xO_{7+x}N_{2-x}$ solids solutions sintered at 1680°C for 4 h a) $Yb_4Si_2O_7N_2$; (b) $Yb_4Si_{2-x}Al_xO_{7+x}N_{2-x}$, $x = 0{\cdot}33$; c) $Yb_4Si_{2-x}Al_xO_{7+x}N_{2-x}$, $x = 1$; d) $Yb_4Si_{2-x}Al_xO_{7+x}N_{2-x}$, $x = 1{\cdot}33$.

Prolonged firings of the samples at 1680°C resulted in enhanced grain growth. Equiaxed rounded grains up to several mm long were obtained after firing periods of 100 h.

The distribution of Yb, Si, Al, O, and N was confirmed to be uniform by WDS mapping performed on polished surfaces of sintered samples. Only in the samples subjected to extended (100 h) annealings, minor amounts (< 1–2 vol%) of a grain boundary phase assemblage segregated in triple points and along grain boundaries were observed. This assemblage appears to have a very fine-grained eutectic structure and is somewhat enriched with Al, but slightly depleted in Si and 0.

Thermal oxidation resistance tests of $Yb_4Si_2O_7N_2$ under non-isothermal (heating rate 2 K min^{-1}) conditions indicated that active oxidation in air starts at slightly below 700°C. Therefore, a temperature of 720°C was chosen for isothermal oxidation tests of all materials.

In the case of pure ytterbium woehlerite, $Yb_4Si_2O_7N_2$, oxidation was accompanied by severe cracking of the samples and their partial or complete disintegration by the time the oxidation was complete. With increasing Al/Si ratio, the samples exhibited both better oxidation resistance and diminished cracking. The latter was almost negligible if not non-existent for the samples with an Si/Al ratio of 1/1, and was not observed for the ones with a 1/2 ratio. The results of the XRD examination of the oxidation products are listed in Table 4.

Table 4. Oxidation products of members of the solid solution series $Yb_4Si_2O_7N_2$–$Yb_4Al_2O_9$ (isothermal oxidation at 720°C for 10 h)[a]

Compound	*Oxidation product*
$Yb_4Si_2O_7N_2$	$Yb_4Si_2O_7N_2$(?),[b] Yb_2O_3
$Yb_4Si_{2-x}Al_xO_{7+x}N_{2-x}$, $x = 0{\cdot}33$	Yb_2SiO_5, $Yb_4Al_2O_9$
$Yb_4Si_{2-x}Al_3O_{7+x}N_{2-x}$, $x = 1$	$Yb_4Al_2O_9$, Yb_2O_3
$Yb_4Si_{2-x}Al_xO_{7-x}N_{2-x}$, $x = 1{\cdot}33$	$Yb_4Al_2O_9$, Yb_2O_3

[a]As determined by XRD; in descending order in accordance with the amount of phase present. Amorphous SiO_2 was detected in all oxidised samples by means of X-ray fluorescent spectrometry (see text).
[b]Either partly decomposed or residual unoxidised woehlerite. The diffractogramm shows very broad reflections with low intensities.

Crystalline silica was not detected by XRD in any of the samples. Therefore, it is believed that silica is present in the oxidation products in an amorphous form as is often observed for Si_3N_4 ceramics and some rare earth oxynitrides under conditions of low-temperature oxidation.[41,42] In fact, the presence of SiO_2 was confirmed by means of semi-quantitative X-ray fluorescence spectroscopy in quantities consistent with the expected SiO_2 formation after complete oxidation of the corresponding materials.

It should be noted that the obviously poor oxidation resistance of the synthesised pure Yb–woehlerite and to a lesser extent of $Yb_4Si_{2-x}Al_xO_{7+x}N_{2-x}$ solid solutions can be partly ascribed to the high porosity (up to 15%) of the samples. The oxidation stability of the dense Si_3N_4-based materials with $RE_4Si_{2-x}Al_xO_{7+x}N_{2-x}$ compounds as secondary intergranular phases (normally not more than several vol%) may prove to be superior and comparable to that of N–melilite solid solutions with alumina ($RE_2Si_{3-x}Al_xO_{3+x}N_{4-x}$,$x \leq 1$).

4 Conclusions

1. A complete solid solution between $Yb_4Si_2O_7N_2$ and $Yb_4Al_2O_9$ with general formula $Yb_4Si_{2-x}Al_xO_{7+x}N_{2-x}$ has been established. Intermediate members exhibit a pseudotetragonal symmetry and obviously indicate non-ideal solid solution behaviour near an Si/Al ratio of around 1/1.
2. Further work should clarify possible O/N and/or Al/Si ordering schemes in the solid solution. Additional investigations are also needed on the possible solid solution range between $RE_4Si_2O_7N_2$ and $RE_4Al_2O_9$ for RE = La, Ce, Pr, and Nd, while keeping in mind that La-, Ce-, and $Pr_4Al_2O_9$ are not stable at any temperature and $Nd_4Al_2O_9$ is only stable in a small temperature range at high temperatures.
3. The space group of $La_4Si_2O_7N_2$, previously given as $P2_1/m$, should be re-investigated and it should be clarified if the correct space group is not in fact $P2_1/c$ as for the other $RE_4Si_2O_7N_2$ compounds.
4. The increase of the amount of Al_2O_3 dissolved in woehlerite noticeably improves oxidation resistance and elevates the temperature of thermal decomposition in nitrogen atmosphere. $Yb_4Si_{2-x}Al_xO_{7+x}N_{2-x}$ solid solutions as grain boundary phases may considerably improve the refractoriness and the high-temperature mechanical properties of silicon nitride-based ceramics, and thus may be as promising as the recently investigated N–melilite solid solutions $RE_2Si_{3-x}Al_xO_{3+x}N_{4-x}$($x \leq 1$).

Acknowledgements

The authors are grateful to Dr Yu. Gogotsi for assistance with the oxidation measurements. The participation of Dr V. A. Ijevskii in this work was supported by Alexander von Humboldt Foundation.

References

1. Clarke, D. R., High-temperature microstructure of a hot-pressed silicon nitride. *J. Am. Ceram. Soc.*, 1989, **72**(9), 1604–1609.
2. Tsai, R. L. and Raj, R., The role of grain–boundary sliding in fracture of hot-pressed Si_3N_4 at high temperatures. *J. Am. Ceram. Soc.*, 1980, **63**(9–10), 513–517.
3. Tsuge, A., Nishida, K. and Komatsu, M., Effect of crystallizing the grain–boundary glass phase on the high-temperature strength of hot-pressed Si_3N_4 containing Y_2O_3. *J. Am. Ceram. Soc.*, 1975, **58**(7–8), 323–326.
4. Clarke, D. L., Lange, F. F. and Schnittgrund, G. D., Strengthening of a sintered silicon nitride by a post-fabrication heat treatment. *J. Am. Ceram. Soc.*, 1982, **65**(4), C51.
5. Cheng, Y.-B. and Thompson, D. P., Aluminum-containing nitrogen melilite phases. *J. Am. Ceram. Soc.*, 1994, **77**(1), 143–148.
6. Chee, K. S., Cheng, Y.-B. and Smith, M. E., The solubility of aluminum in rare earth nitrogen melilite phases. *J. Eur. Ceram. Soc.*, 1995, **15**, 1213–1220.
7. Mandal H., Cheng Y.-B. and Thompson D. P., α-Sialon ceramics with a crystalline melilite grain–boundary phase. In *Proceedings of the 5th International Symposium, Ceramic Materials and Components for Engines*, Shanghai 1994, eds. D. S. Yan, X. R. Fu, and S. X. Shi. World Scientic, Singapore, 1995, pp. 202–205.
8. Wang, P. L., Tu, H. Y., Sun, W. Y., Yan, D. S., Nygren, M. and Ekström, T., Study on the solid solubility of Al in the melilite system $R_2Si_{3-x}AlxO_{3+x}N_{4-x}$ with R = Nd, Sm, Gd, Dy and Y. *J. Eur. Ceram. Soc.*, 1995, **15**, 689–695.
9. Camuscu, N., Mandal, H. and Thompson, D. P., Optimised high-temperature sialon ceramics containing melilite as the grain boundary phase. In *21st Century Ceramics, British Ceramics Proceedings, 1996*, **55**, pp. 239–248, ed. D. P. Thompson and H. Mandal. The Institute of Materials, London.
10. Huang Z.-K., Chen I.-W., Rare-earth melilite solid solution and its phase relations with neighbouring phases. *J. Am. Ceram. Soc.*, 1996, **79**(8), 2091–2097.
11. Marchand, R., Jajaveera, A., Verdier, P. and Lang, J., Preparation and characterization of new oxynitrides in the system Ln–Si–O–N. The melilites $Ln_2Si_3O_3N_4$ and the cuspidines $Ln_4Si_2O_7N_2$. *C. R Acad. Sci. Paris, Ser. C*, 1976, **C283**, 675–677 (in French).
12. Thompson, D. P., The crystal chemistry of nitrogen ceramics. *Mater. Sci. Forum*, 1989, **47**, 21–42.
13. MacKenzie, K. J. D., Gainsford, G. J. and Ryan, M. J., Rietveld refinement of the crystal structures of the yttrium silicon oxynitrides $Y_2Si_3N_4O_3$ (N–Melilite) and $Y_4Si_2O_7N_2$ (J-phase). *J. Eur. Ceram. Soc.*, 1996, **16**, 553–560.
14. International Center for Diffraction Data, JCPDS-Powder Diffraction File, Sets 1-44, Park Lane, Swarthmore, PA.

15. Benoit, P. H., Adaptation to microcomputer of the Appleman–Evans program for indexing and least-squares refinement of powder-diffraction data for unit cell dimensions. *Am. Miner.*, 1987, **72**, 1018–1019.
16. Appleman, D. E. and Evans, H. T., Jr, Job 9214: indexing and least-square refinement of powder diffraction data. *US Geological Survey, Computer contribution 20*, US Technical Information Service, Document PB2-16188, 1973.
17. Thompson, D. P., Phase relationships in Y–Si–Al–O–N ceramics, In *Proceedings Tailing Multiphase and Composite Ceramics*, ed. R. E. Tressler, G. L. Messing, C. G. Patano, and R. E. Newnham, 1986, pp. 79–91.
18. Nishimura, T. and Mitomo, M., Phase relationships in the system Si_3N_4–SiO_2–Yb_2O_3. *J. Mater. Res.*, 1995, **10**(2), 240–242.
19. Thompson, D. P., On ordering in oxynitride ceramics. *Euro-Ceramics II, Proceedings of the Second European Ceramic Society Conference*, 11–14 September 1991, Augsburg, Germany, Vol. 1, ed. G. Ziegler and H. Hausner, Deutsche Keramische Gesellschaft, Germany, 1991.
20. Baraton, M. I., Marchand, R. and Quintard, P., Preliminary study of some 'pyro'-silico-nitrides. *Journal of Molecular Structure*, 1984, **115**, 91–94.
21. Morgan, P. E. D., Comment on the structures of $Ce_4Si_2O_7N_2$, $La_4Si_2O_7N_2$, '$Ce_2O_3 \cdot 2Si_3N_4$' and '$La_2O_3 \cdot 2Si_3N_4$'. *J. Am. Ceram. Soc.*, 1979, **62**, 636.
22. Guha, J. P., The crystal structure of the silicon cerium oxynitride, $Ce_4Si_2O_7N_2$. *J. Mater. Sci.*, 1980, **15**, 262–263.
23. Lang, J., Silicate structures and atomic substitution, In *Progress in Nitrogen Ceramics*, ed. F. L. Riley, pp. 23–43. NATO ASI Series E: Applied Sciences, No. 65. Martinus Nijhoff, Boston, MA, 1983.
24. Marchand, R., Laurent, Y., Guyader, J., L'Haridon, P. and Verdier, P., Nitrides and oxynitrides: preparation, crystal chemistry and properties. *J. Eur. Ceram. Soc.*, 1991, **8**, 197–213.
25. Thompson, D. P., New grain–boundary phases for nitrogen ceramics. *Mat. Res. Soc. Symp. Proc.*, 1993, **287**, 79–92.
26. Montorsi, M. and Appendino, P., Silicon lanthanide oxinitrides of the $M_4Si_2O_7N_2$ type. *J. Less-Comm. Met.*, 1979, **68**, 193–197.
27. Merlino, S. and Perchiazzi, N., Modular mineralogy in the cuspidine group of minerals. *Can. Miner.*, 1988, **26**, 933–943.
28. Wills, R. R., Stewart, R. W., Cunningham, J. A. and Wimmer, J. M., The silicon lanthanum oxynitrides. *J. Mater. Sci.*, 1976, **11**, 749–759.
29. Ii, N., Mitomo, M. and Inoue, Z., Single-crystal growth of $La_4Si_2O_7N_2$ by the floating zone method. *J. Mater. Sci.*, 1980, **15**, 1691–1695.
30. Mitomo, M., Izumi, F., Horiuchi, S. and Matsui, Y., Phase relationships in the system Si_3N_4–SiO_2–La_2O_3. *J. Mater. Sci.*, 1982, **17**, 2359–2364.
31. Cao, G.-Z., Huang, Z.-K. and Yan, D.-S., Phase relationships in the Si_3N_4–Y_2O_3–La_2O_3 system. *Science in China, Ser. A*, 1989, **32**, 429–433.
32. Mizuno, M. and Yamada T., Formation and some properties of binary compounds in lanthanide oxide–aluminum oxide systems. *Nagoya Kogyo Gijutsu Shikensho Hokoku*, 1990, **39**(4), 156–175 (in Japanese).
33. Kolitsch, U., On the constitution of the systems of rare earths, yttria, and scandia with SiO_2, Al_2O_3, and MgO. Diploma thesis, University of Stuttgart, Germany, 1992 (in German).
34. Wu, P. and Pelton, A. D., Coupled thermodynamic-phase diagram assessment of the rare earth oxide–aluminium oxide binary systems. *J. Alloys and Compounds*, 1992, **179**, 259–264.
35. Sun, W. Y., Yan, D. S., Gao, L., Mandal, H., Liddell, K. and Thompson, D. P., Subsolidus phase relationships in systems Ln_2O_3–Si_3N_4–AlN–Al_2O_3 (Ln = Nd, Sm). *J. Eur. Ceram. Soc.*, 1995, **15**, 349–355.
36. Kolitsch, U., Seifert, H. J. and Aldinger, F., to be submitted to *Z. Metallkd.*
37. Seifert, H. J., Kolitsch, U. and Aldinger, F., in preparation.
38. Neidhardt, U., Schubert, H., Bischoff, E. and Petzow, G., Gas pressure sintering of Si_3N_4 in N_2/CO/(CO_2) atmosphere. In *Proceedings of the International Conference on Silicon Nitride-based Ceramics*, Stuttgart, 4-6 October 1993, pp. 187–192.
39. Mitra, S., Dutta, G. and Dutta, I., Effect of heat treatment on the microstructure and properties of dense AlN sintered with Y_2O_3 additions. *J. Am. Ceram. Soc.*, 1995, **78**(9), 2335–2344.
40. Yamane, H., Ogawara, K., Omori, M. and Hirary, T., Phase transition of rare-earth aluminates ($RE_4Al_2O_9$) and rare-earth gallates ($RE_4Ga_2O_9$). *J. Am. Ceram. Soc.*, 1995, **78**(9), 2385–2390.
41. Veyret, J.-B., Van de Voorde, M. and Billy, M., Oxidation behavior of silicon yttrium oxinitride. *J. Am. Ceram. Soc.*, 1992, **75**(12), 3289–3292.
42. Mizuno, M. and Noguchi, T., Phase diagram of the system aluminum oxide–ytterbium (III) oxide at high temperatures. *Yogyo Kyokai Shi*, 1980, **88**(6), 322–327 (in Japanese).